A Ciliary SMOOTHENED-GRK2-PKA Signaling Pathway Initiates Hedgehog Signal Transduction

Madison F. Walker[1, 2, 3 ,13], Jingyi Zhang[4,13], William Steiner[1, 2, 3, 13], Pei-I Ku[5, 13], Ju-Fen Zhu[1, 2, 3], Zachary Michaelson[1, 2, 3], Yu-Chen Yen[6], Alyssa B. Long[7], Mattie J. Casey[1], Abhishek Poddar[5], Isaac B. Nelson[1, 2, 3], Corvin D. Arveseth[1, 2, 3, 8], Falko Nagel[9], Ryan Clough[10], Sarah LaPotin[10], Kristen M. Kwan[10], Stefan Schulz[9,11], Rodney A. Stewart[1], John J. G. Tesmer[6,12], Tamara Caspary[7], Radhika Subramanian[5,*], Xuecai Ge[4,*], Benjamin R. Myers[1, 2, 3,14,*]

[1] Department of Oncological Sciences, Huntsman Cancer Institute, University of Utah School of Medicine, Salt Lake City UT 84112 USA
[2] Department of Biochemistry, University of Utah School of Medicine, Salt Lake City UT 84112 USA
[3] Department of Bioengineering, University of Utah School of Medicine, Salt Lake City UT 84112 USA
[4] Department of Molecular and Cell Biology, School of Natural Sciences, University of California, Merced, CA, USA
[5] Department of Molecular Biology, Massachusetts General Hospital, Boston, MA 02114 USA; Department of Genetics, Harvard Medical School, Boston, MA 02115 USA
[6] Department of Biological Sciences, Purdue University, West Lafayette, IN, USA
[7] Department of Human Genetics, Emory University School of Medicine, Atlanta, GA 30322, USA
[8] Present address: Medical Scientist Training Program, Washington University School of Medicine, St. Louis, MO USA
[9] 7TM Antibodies GmbH, Jena, Germany
[10] Department of Human Genetics, University of Utah School of Medicine, Salt Lake City UT 84112 USA
[11] Institute of Pharmacology and Toxicology, University Hospital Jena, Jena, Germany
[12] Department of Medicinal Chemistry and Molecular Pharmacology, Purdue University, West Lafayette, IN, USA
[13] co-first author
[14] Lead contact

* Correspondence: radhika@molbio.mgh.harvard.edu (R.S.); xge2@ucmerced.edu (X.G.); benjamin.myers@hci.utah.edu (B.R.M.)

ABSTRACT:

During Hedgehog (Hh) signal transduction in development, homeostasis, and cancer, the atypical G protein-coupled receptor (GPCR) SMOOTHENED (SMO) communicates with GLI transcription factors by directly binding the PKA catalytic subunit (PKA-C) and physically blocking its enzymatic activity. Here we show that GPCR kinase 2 (GRK2) orchestrates this process during endogenous Hh signal transduction in the vertebrate primary cilium. Hh pathway activation triggers rapid GRK2 relocalization from the base to the shaft of the cilium, leading to SMO phosphorylation and ultimately formation of SMO / PKA-C complexes in this compartment. *In vitro* reconstitution experiments reveal that GRK2 phosphorylation is sufficient to trigger direct binding of the SMO active conformation to PKA-C, without participation from additional proteins. Lastly, the SMO-GRK2-PKA communication pathway operates during Hh signaling in a range of cellular and *in vivo* models. Our work highlights GRK2 phosphorylation of ciliary SMO as a key initiating event for the intracellular steps of the Hh cascade, enabling a deeper understanding of how Hh signals are transduced intracellularly in tissues and organs to orchestrate proliferative and differentiative decisions. More broadly, our study hints at an expanded role for GRKs in enabling direct GPCR interactions with a diverse array of intracellular effectors.

INTRODUCTION:

The Hedgehog (Hh) signaling pathway is a cornerstone of animal development and disease, controlling the formation of nearly every vertebrate organ and instigating several common malignancies[1–6]. To carry out these roles, the Hh pathway utilizes an intracellular transduction cascade that originates at the cell surface and propagates to the nucleus, culminating in transcription of genes linked to proliferation or differentiation[1–4]. This process relies on the primary cilium, a tiny antenna-shaped cell surface compartment thought to facilitate the underlying biochemical steps via its highly confined ultrastructure and its unique protein and lipid inventory[7–10]. Despite extensive research, the mechanisms by which Hh signals are transmitted from the cell surface to the nucleus remain longstanding mysteries[1–4].

In the Hh pathway "off" state, the atypical G protein-coupled receptor (GPCR) SMOOTHENED (SMO) is inhibited within the cilium by PATCHED1 (PTCH1), a 12-transmembrane (TM) sterol transporter that restricts access of SMO to endogenous activating sterol ligands[2–4]. Consequently, SMO is rapidly cleared from the cilium via ubiquitylation and engagement of ciliary exit machinery[11–13], and the protein kinase A catalytic subunit (PKA-C) is free to phosphorylate and inactivate GLI transcription factors[14–21]. In the pathway "on" state, Hh proteins bind to and inhibit PTCH1, enabling SMO to bind sterols[22–25], assume an active conformation[22–25], and accumulate to high levels in the cilium[26–28]. Active SMO blocks PKA-C phosphorylation of GLI, leading to GLI activation[18,20,21,29,30]. SMO inhibition of PKA-C is thus fundamental to Hh signal transduction, but the underlying mechanism has remained poorly understood, mainly because it does not rely on the standard signaling paradigms employed by nearly all other GPCRs[31–33].

We recently discovered that SMO can inactivate PKA-C via an unusual mechanism: it utilizes a decoy substrate sequence, termed the "protein kinase inhibitor" (PKI) motif", to directly bind the PKA-C active site and physically block its enzymatic activity. SMO can bind and inhibit PKA-C as a decoy substrate *in vitro*, and these decoy substrate interactions are necessary for Hh

signal transduction in cultured cells and *in vivo.* Based on these findings, we proposed that SMO utilizes its PKI motif to inactivate PKA-C in cilia, thereby blocking GLI phosphorylation and triggering GLI activation[34,35].

The above model immediately raises a fundamental question: what controls SMO / PKA-C interactions such that they occur only when SMO is in an active state, an essential condition for faithful Hh signal transmission and for avoiding pathological outcomes resulting from insufficient or excessive GLI activation? Indeed, we found that during Hh signal transduction in cilia, only the active, agonist-bound conformation of SMO is competent to colocalize with PKA-C[35]. To explain this phenomenon, we previously proposed that GPCR kinase (GRK) 2 (along with its paralog, GRK3, hereafter referred to collectively as "GRK2") regulate SMO / PKA-C interactions[34,35]. GRKs are a multigene family that bind selectively to the active conformations of GPCRs and phosphorylate the receptor's intracellular domains, triggering interactions between GPCRs and other signaling proteins[36–38]. In support of this proposal, GRK2 is essential for SMO-GLI communication[39–41], and this kinase selectively phosphorylates active, agonist-bound SMO expressed in HEK293 cells[34,42], thereby enhancing interactions between the SMO PKI motif and PKA-C[34,35]. Furthermore, blocking GRK2 kinase activity[39,40] or mutating the GRK2 phosphorylation sites on SMO[34], which we mapped via mass spectrometry[34], reduces SMO / PKA-C interactions in HEK293 cells[34] and blocks Hh signal transduction *in vivo*[39,40].

Although these findings suggest that GRK2 may serve as an intermediary between SMO and PKA-C, they leave the physiological relevance of the SMO-GRK2-PKA communication pathway, as well as its underlying molecular mechanism, unresolved in several respects. First, whether SMO undergoes GRK2-mediated phosphorylation during physiological Hh signal transduction in the primary cilium is unclear. Whereas all other essential Hh pathway components localize in or near the cilium[16,26–28,43], whether this is true for GRK2 remains unknown. In addition, our strategy to identify GRK2 phosphorylation sites on SMO has limitations, as it involved overexpression of a truncated, stabilized SMO in a non-ciliated cell line, and utilized biochemical

detection methods that lack subcellular resolution[34]. Consequently, GRK2 phosphorylation of SMO, and its role in SMO / PKA-C interactions, have not been studied during endogenous Hh signal transduction on physiologically relevant time scales in primary cilia. Second, while GRK2 phosphorylation contributes to formation of SMO / PKA-C complexes[34], it remains unclear whether phosphorylation directly triggers SMO to bind PKA-C, or whether the effect of GRK2 phosphorylation requires additional proteins. This is a critical question because GRK2 phosphorylation of GPCRs is canonically associated with binding of β-arrestins[36–38], and has not been previously demonstrated to induce direct interactions between a GPCR and PKA-C. Finally, our new model for SMO / PKA-C communication has only been evaluated in cultured fibroblasts and zebrafish somitic muscle *in vivo*[34,35]. Thus, we do not yet know whether the SMO-GRK2-PKA pathway is a general aspect of Hh signaling beyond these specific systems.

Here we address these knowledge gaps by developing novel imaging modalities and immunological detection reagents to monitor the SMO-GRK2-PKA pathway in physiological models of Hh signal transduction, along with *in vitro* reconstitution strategies to dissect its underlying biochemical mechanisms. Using these approaches, we show that SMO, upon activation, undergoes rapid phosphorylation by a pool of GRK2 recruited from the base to the shaft of the cilium, enabling formation of ciliary SMO / PKA-C complexes. We also find that GRK2 phosphorylation is sufficient to trigger direct SMO / PKA-C interactions in a purified *in vitro* system with no other proteins present. Finally, we demonstrate that SMO undergoes GRK2-mediated phosphorylation during Hh signal transduction in multiple tissue, organ, and animal settings. Our work establishes GRK2 phosphorylation of ciliary SMO, and the ensuing PKA-C recruitment, as critical initiating events for transmission of Hh signals from the cell surface to the nucleus. Furthermore, our work provides a blueprint to study the cell biological basis for SMO-PKA communication and other GRK-dependent signaling cascades throughout development, physiology, and disease.

RESULTS:

GRK2 relocalizes from the base to the shaft of the cilium upon SMO activation

If SMO undergoes GRK2 phosphorylation during Hh signal transduction, then GRK2 should be detectable in or near the cilium. Initial attempts to visualize GRK2 in the cilium via immunofluorescence were confounded by an abundant GRK2 signal in the cell body (data not shown). Because kinase-substrate interactions are typically transient and dynamic[44,45], we suspected that sensitive imaging methods capable of tracking GRK2 localization over extended time periods might reveal patterns of transient, low-level ciliary localization over the high "background" GRK2 signal emanating from the cell body.

We therefore established a live-cilium total internal reflection fluorescence (TIRF) microscopy method to study dynamic protein localization to the cilium over long (multi-hour) time intervals (Fig. 1A). We stably expressed a GRK2-eGFP fusion in inner medullary collecting duct (IMCD3) cells, a well-established cultured cell model for ciliary imaging studies[34,46,47], and labeled cilia with a live-cell tubulin dye (SiR Tubulin) (Fig. 1B). To select cells for TIRF studies, eGFP-positive cells were imaged for 15 minutes prior to addition of SAG21k (a high-affinity derivative of the SMO agonist SAG). Only cells exhibiting stable ciliary attachment to the coverslip surface during this period were imaged and analyzed further (n=150). TIRF imaging revealed a punctate GRK2-eGFP signal at the ciliary base in 142 cells (~95%) prior to SAG21k treatment (Fig. 1C-D, Supplementary Movie 1). Following addition of SAG21k, a faint but reproducible eGFP signal appeared along the entire ciliary shaft in approximately 53% (79/150) of cells, consistent with GRK2 recruitment to activated SMO within the cilium (Fig. 1C-D, Supplementary Movie 1). GRK2-eGFP was detectable as early as 3 minutes following SAG21k treatment in some cases, although the kinetics of varied between cilia (from 3 to 105 min, median = 21 min) (Fig. 1E). We suspect that the variability arises due to challenges in detecting the low GFP signal in the cilium relative to background fluorescence in the cell body, rather than intrinsic variability in the kinetics of GRK2 ciliary localization themselves. Once GRK2-eGFP appeared in cilia, it persisted for several hours

thereafter (the duration of the imaging experiment) (Fig. 1C), indicating that SMO activation elicits a sustained, steady-state redistribution of GRK2 from the base to the shaft of the cilium.

Thus, our cilium TIRF imaging studies reveal a pool of GRK2 that localizes to the ciliary base and rapidly redistributes into the ciliary shaft upon SMO activation. These findings are consistent with GRK2 recognition of the SMO active conformation as an early event in intracellular transmission of Hh signals.

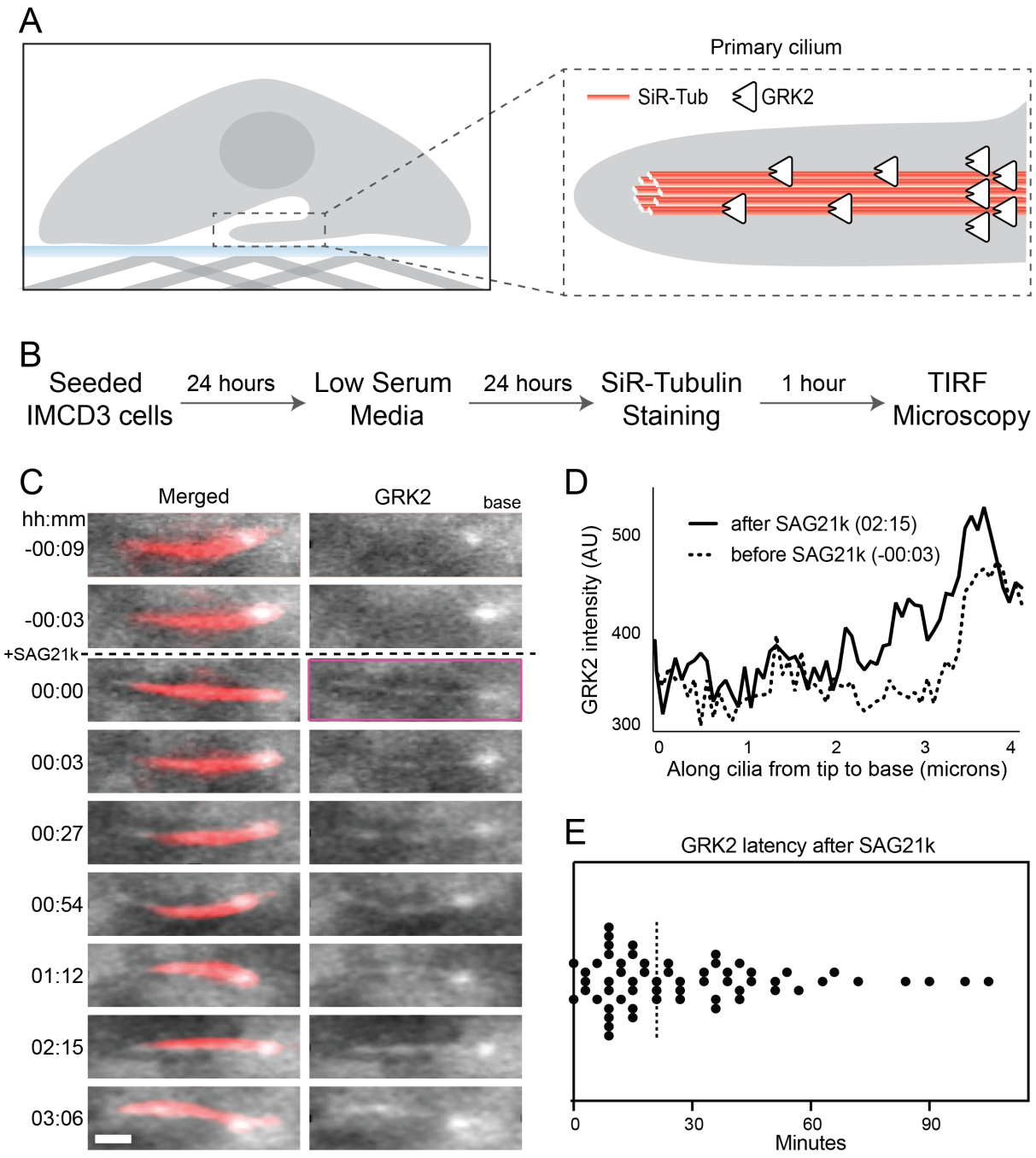

Fig 1: GRK2 relocalizes from the base to the shaft of the cilium upon SMO activation

(A) Schematic illustration of a cell with the cilium attached to the coverslip surface for TIRF imaging (left). A close-up view of the cilium (right) where the microtubule was labeled with SiR-Tub and GRK2-eGFP was stably expressed. **(B)** Flowchart outlining the sample preparation procedures for imaging. **(C)** Representative montage from live-cell imaging of a cilium. Merged (red = SiR-Tubulin and gray = GRK2-eGFP) and GRK2-eGFP channels are shown. SMO was activated at t = 00:00 (hh:mm) by adding SAG21k. The montages show that eGFP signal was observed in the base of the cilium. After SAG21k addition, eGFP signal is observed in the shaft,

and the signal persists for the duration of imaging. (Scale bar = 1 μm). **(D)** GRK2-eGFP intensity profiles before and after SAG21k activation, for the cilium in (C). **(E)** Scatterplot of the GRK2 latency, defined as the time after SAG21k addition when a GRK2-eGFP signal was observed in the cilium; dashed line indicates median.

Hh pathway activation leads to accumulation of GRK2-phosphorylated SMO in the cilium

Our GRK2 localization studies suggest that SMO undergoes GRK2-mediated phosphorylation within the cilium. To detect these phosphorylation events directly, we raised a phospho-specific antibody (hereafter referred to as "anti-pSMO") by immunizing rabbits with a phosphorylated peptide spanning a cluster of highly conserved GRK2 sites that we previously defined in the SMO intracellular membrane-proximal cytoplasmic tail (pCT) (S594, T597, and S599)[34] (Fig. 2A). Characterization of our anti-pSMO antibody in transfected HEK293 cells demonstrated that it stringently and specifically recognizes the active, GRK2-phosphorylated form of SMO (Fig S2A-C).

We turned to NIH3T3 fibroblasts to study GRK2 phosphorylation of endogenous SMO in its native ciliary context. These cells are widely considered the "gold standard" cultured cell model for Hh signal transduction, as they efficiently form cilia and endogenously express all pathway components required to transmit Hh signals from the cell surface to the nucleus[26,27,48,49]. In the Hh pathway "off" state, we did not observe SMO phosphorylation in cilia, as assessed via immunofluorescence microscopy with the anti-pSMO antibody (Fig. 2B). In contrast, endogenous SMO is phosphorylated in cilia following Hh pathway activation using SAG21k (Fig. 2B, Fig. S2D) or the N-terminal signaling fragment of Sonic hedgehog (ShhN) (Fig. S2D). This ciliary signal was absent in *Smo*$^{-/-}$ fibroblasts (Fig. S2E), demonstrating that the anti-pSMO antibody specifically detects endogenous phosphorylated SMO in cilia. The anti-pSMO signal colocalized with the signal from an anti-SMO antibody that stains the ciliary base and shift regions (and recognizes SMO regardless of phosphorylation state), suggesting that phosphorylated SMO localizes throughout the cilium. Ciliary anti-pSMO staining in NIH3T3 cells was abolished by treatment with one of two chemically distinct GRK2 inhibitors, Cmpd101 or 14as[50] (Fig. 2B, S2F). The effects of GRK2 inhibition were not attributable to changes in SMO ciliary localization, since total SMO in cilia remained constant following treatment with the GRK2 inhibitors (Fig. 2B, S2F). This finding is consistent with previous observations that GRK2 inhibitors block Hh signal transduction in

mouse fibroblasts without affecting levels of SMO in cilia[39–41]. Thus, GRK2 controls SMO phosphorylation during endogenous Hh signal transduction in cilia, at least at the site(s) recognized by our anti-pSMO antibody.

Prior studies have implicated the α and ɣ isoforms of casein kinase 1 (CK1) in SMO phosphorylation[51,52]. These studies initially proposed SMO S594/T597/S599 as CK1 phosphorylation sites, based an *in vitro* phosphorylation assay involving purified CK1α and a soluble construct encompassing the full-length, unstructured SMO cytoplasmic domain[51]. However, compound D4476, which potently inhibits all CK1 isoforms[53–55], failed to decrease SAG21k-induced phosphorylation of endogenous full-length SMO in NIH3T3 cilia (Fig 2B), indicating that CK1 does not phosphorylate SMO S594/T597/S599 under physiological conditions.

We considered whether ciliary SMO phosphorylation arises simply from SMO ciliary localization, rather than SMO activation. To distinguish between these possibilities, we uncoupled SMO ciliary trafficking from activation using NIH3T3 cells stably expressing of a short hairpin RNA against the dynein 2 heavy chain (hereafter referred to as NIH3T3 *dync2* cells)[28,56]. NIH3T3 *dync2* cells harbor high levels of inactive SMO in cilia, even in the pathway "off" state[28,56] (Fig 2C). If phosphorylation were a result of SMO localization in cilia, it should occur in NIH3T3 *dync2* cells without Hh pathway activation. However, we did not detect phosphorylated SMO in vehicle-treated NIH3T3 *dync2* cells, whereas SAG21k treatment strongly induced SMO phosphorylation (Fig. 2C). Furthermore, treatment of wild-type NIH3T3 cells with the SMO inverse agonist cyclopamine, which causes SMO to accumulate in cilia in an inactive conformation[28,57,58], also failed to induce SMO phosphorylation (Fig. 3A). Thus, SMO must be in an active conformation to undergo GRK2 phosphorylation in the cilium.

To validate the findings from our microscopy studies, we examined SMO phosphorylation in NIH3T3 cells via immunoblotting. Because the anti-pSMO antibody was not sufficiently sensitive to detect phosphorylation of endogenous SMO (Fig. 2D, "parental"), we generated an

NIH3T3 line stably expressing low levels of FLAG-tagged SMO for these studies, thereby minimizing possible overexpression artifacts. Control experiments confirmed that the stably expressed FLAG-SMO, like its endogenous counterpart, underwent physiological regulation by ciliary trafficking machinery (Fig. S2F). FLAG-SMO exhibited low but detectable basal phosphorylation that was strongly increased by SAG21k, and this effect was abolished by Cmpd101 (Fig. 2D, "FLAG-SMO"). We note that FLAG-SMO levels increase modestly following SMO activation, consistent with observations regarding endogenous SMO[57]. However, after measuring the normalized ratio of phosphorylated to total SMO in each condition, we conclude that this modest increase in FLAG-SMO levels cannot explain the dramatic effects of SMO agonist or GRK2 inhibitor on SMO phosphorylation that we observed (Fig 2D).

Together, our immunofluorescence and immunoblotting studies demonstrate that active SMO undergoes GRK2-dependent phosphorylation in ciliated cultured cells.

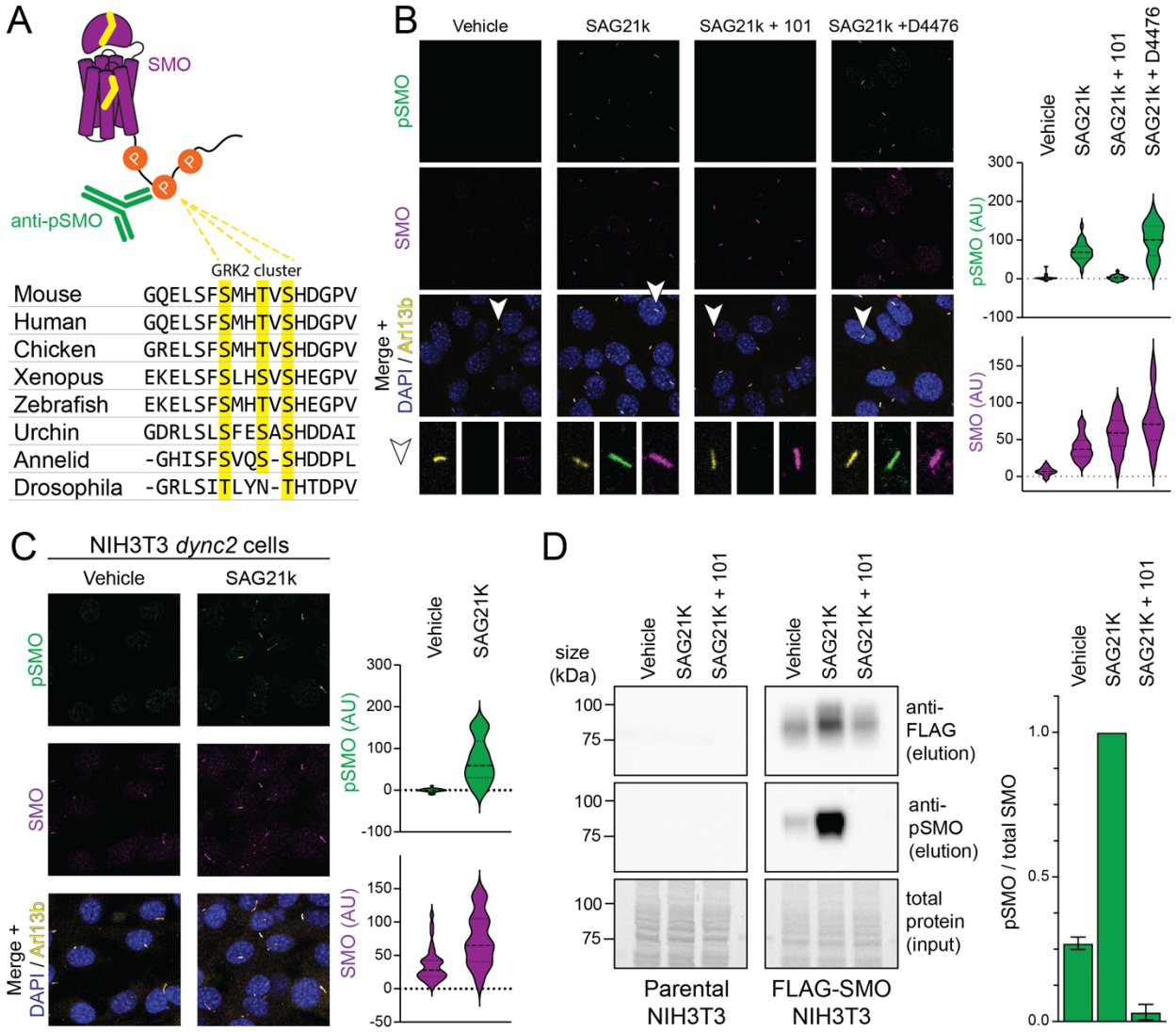

Figure 2: Hh pathway activation leads to accumulation of GRK2-phosphorylated SMO in the cilium.

(A) Alignment of a region of the SMO pCT from various species, with the yellow highlighted residues indicating the conserved GRK2 phosphorylation cluster recognized by our anti-pSMO antibody (see "Methods"). **(B)** NIH3T3 cells were treated overnight with SAG21k (500 nM) in the presence or absence of the GRK2 inhibitor Cmpd101 (101, 30 μM) or the casein kinase 1 inhibitor D4476 (10 μM), or with a vehicle control. Cells were then fixed and stained with anti-pSMO (green), anti-SMO (magenta), anti-Arl13b (to mark cilia, yellow), and DAPI (to mark nuclei, blue). Representative cilia (arrowhead) are highlighted below each image. **(C)** NIH3T3 *dync2* cells were treated with SAG21k or a vehicle control, then stained and quantified as in (B). **(D)** NIH3T3 cells stably expressing FLAG-tagged SMO (right) or parental controls (left) were treated for four hours with vehicle, SAG21k, or SAG21k plus Cmpd101, as described in (B), then lysed and subject to FLAG immunoaffinity chromatography. FLAG eluates were blotted with anti-pSMO and anti-FLAG to detect phosphorylated SMO and total SMO, respectively. The total protein from the input fractions (prior to FLAG chromatography) serve as loading controls. Left: raw data, Right: quantification (mean +/- standard deviation from two independent experiments.)

GRK2 phosphorylation of ciliary SMO is an early event in Hh signal transmission

During Hh signal transduction, key pathway steps downstream of SMO, such as post-translational modification of GLI proteins and GLI accumulation at the cilium tip, begin to occur within 1-2 hours of SMO activation[18,20,59]. In contrast, the kinetics of SMO phosphorylation and SMO / PKA-C interaction in primary cilia are unknown. We used our anti-pSMO antibody to assess whether SMO undergoes phosphorylation in cilia on a time scale consistent with established Hh pathway signaling events.

In initial experiments, we observed SMO phosphorylation in NIH3T3 cilia starting one hour after pathway activation (Fig. 3A). However, these measurements likely underestimate the speed of ciliary SMO phosphorylation because SMO is present at extremely low levels in cilia during the initial phases of Hh pathway activation and requires several hours to accumulate to high levels in this compartment[27,28]. Our experiments might therefore fail to capture SMO phosphorylation at early time points when SMO levels are below the threshold for reliable detection.

To circumvent this issue, we used two independent strategies to enable detection of SMO phosphorylation at early stages of Hh pathway activation, and thereby unmask the true kinetics of SMO phosphorylation in cilia. Critically, both approaches rely on endogenous SMO protein, thereby avoiding potential pitfalls of overexpression-based strategies. First, we treated NIH3T3 cells with cyclopamine to trap SMO in an inactive, nonphosphorylated state in cilia[28,35,57,58], then rapidly activated SMO by replacing cyclopamine with the SMO agonist SAG. Using this approach, we detected SMO phosphorylation in cilia after only 10 minutes of SAG treatment (Fig 3B). Second, in NIH3T3 *dync2* cells, which display some degree of SMO ciliary localization even in the pathway "off" state[28,56] (Fig 2C), we detected SMO phosphorylation in cilia within 5 minutes of SAG21k treatment (Fig S3A). Thus, ciliary SMO undergoes phosphorylation within minutes of Hh pathway activation, consistent with a role for SMO phosphorylation in initiating the intracellular steps of Hh signal transduction.

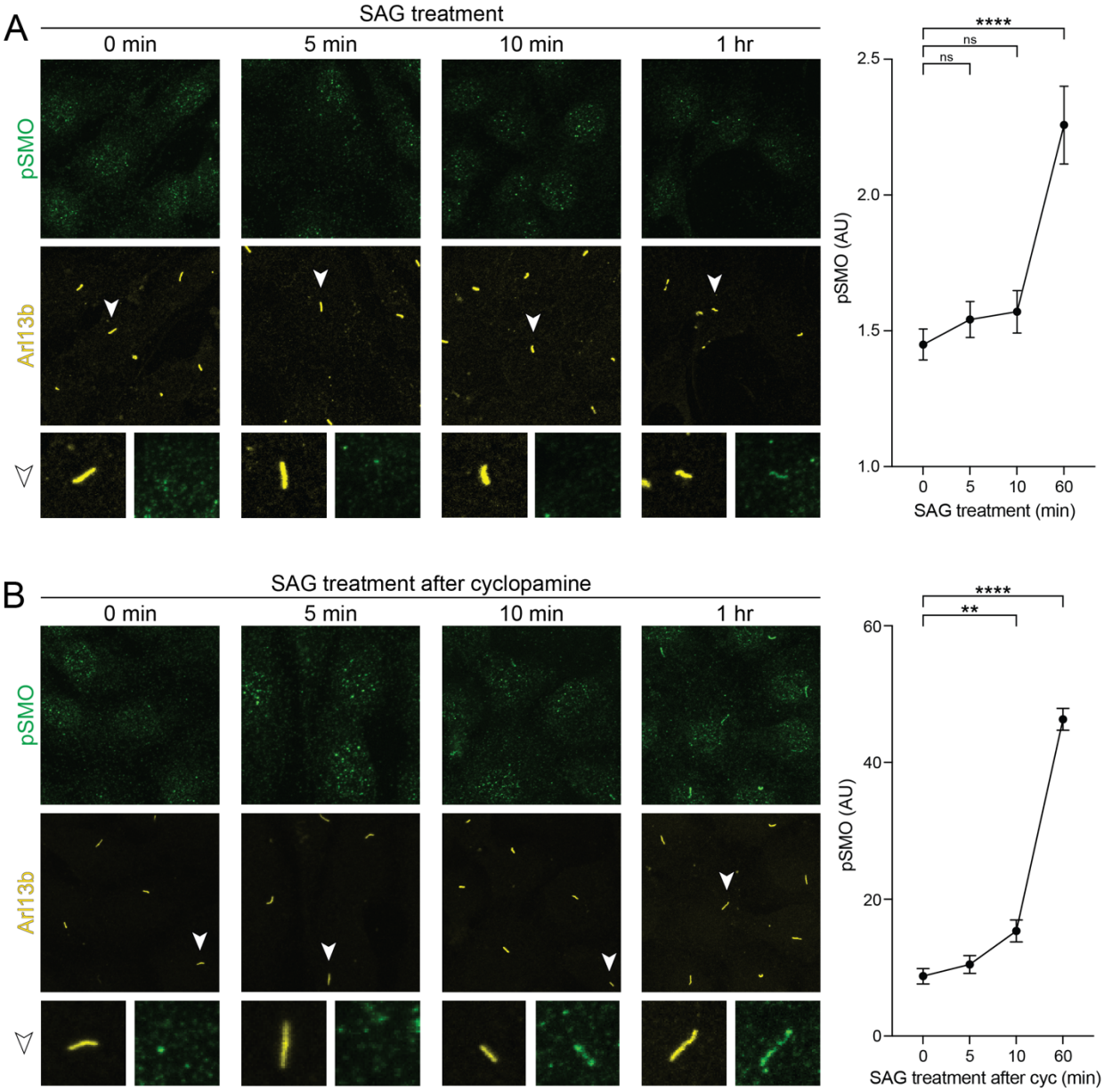

Figure 3: GRK2 phosphorylation of ciliary SMO is an early event in intracellular Hh signal transmission

(A) Left: Wild-type NIH3T3 cells were treated with 100 nM SAG for times ranging from 5 minutes to 1 hour, then fixed and stained for pSMO (green) and Arl13b (yellow). Right: quantification of the mean pSMO intensity in cilia at each indicated time point. **(B)** The same experiment was performed, except NIH3T3 cells were first pretreated with 5μM cyclopamine overnight, followed by SAG treatment as described in (A).

Continuous GRK2 activity sets the SMO phosphorylation state.

Once SMO is activated and undergoes GRK2-mediated phosphorylation, it may persist in a phosphorylated state within the cilium for many hours, without requiring additional GRK2 activity for maintenance. Alternatively, phosphorylation may be dynamic and labile, requiring continuous GRK2 kinase activity to maintain the pool of ciliary SMO in its phosphorylated state. To distinguish between these possibilities, we utilized Cmpd101 to determine how blockade of GRK2 kinase activity impacts the amount of phosphorylated SMO. In immunofluorescence microscopy, SAG21k-induced phosphorylation of ciliary SMO decreased rapidly following Cmpd101 treatment, reaching half-maximal intensity after 15 minutes and returning to baseline levels by 2 hours (Fig 4A). Cmpd101 induced an even faster disappearance of phosphorylated SMO in immunoblotting studies, reaching half-maximal intensity after 5 minutes and nearly undetectable levels at 30 minutes (Fig 4B). These studies indicate that continuous GRK2 kinase activity maintains the pool of ciliary SMO in a phosphorylated state.

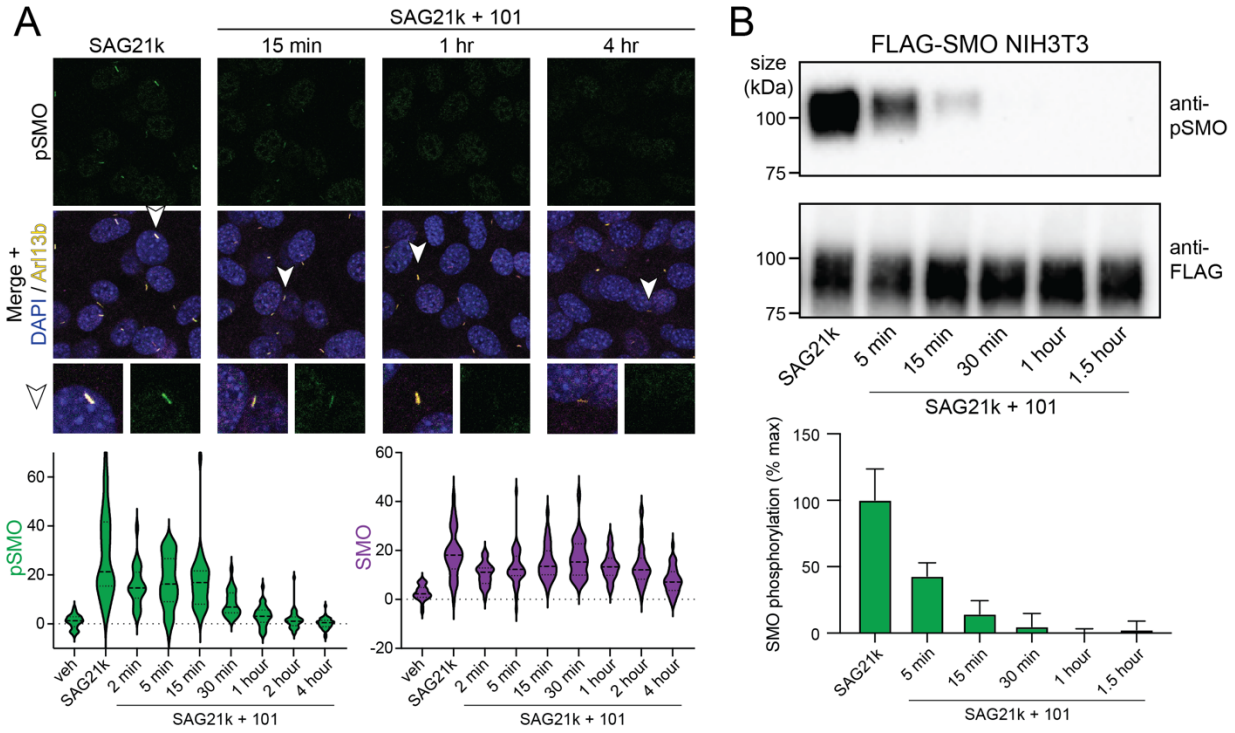

Figure 4: Continuous GRK2 activity sets the SMO phosphorylation state
(A) NIH3T3 cells were treated overnight with SAG21k (500 nM) (left-most panel), and then Cmpd101 (101, 30 μM) was added for the indicated times. Cells were then fixed and stained for pSMO (green), SMO (magenta), Arl13b (yellow), and DAPI (blue), as described in Fig. 2A. Quantification of pSMO and total SMO at the indicated time points are shown below. **(B)** NIH3T3 cells stably expressing FLAG-tagged SMO were treated as in (A), then SMO was purified using FLAG affinity chromatography and the eluates blotted with anti-pSMO and anti-FLAG antibodies. Graph below indicates quantification of band intensities, showing the mean +/- standard deviation from two independent experiments.

GRK2 phosphorylation controls SMO / PKA-C interaction in cilia

Given that SMO undergoes activity-dependent GRK2 phosphorylation in cilia, we next asked whether GRK2 phosphorylation precedes and is required for interaction with PKA-C in this organelle. The amount of PKA-C in cilia is vanishingly small, based on microscopy and proximity-based mass spectrometry measurements[35,46,60,61]. To facilitate PKA-C detection in cilia, we therefore increased the amount of its key interacting partner, SMO, in the ciliary membrane by utilizing a stable NIH3T3 cell line expressing V5-TurboID-tagged SMO at low levels[35]. In this cell line, SAG-bound SMO colocalizes with PKA-C in cilia but cyclopamine-bound SMO does not, confirming that SMO / PKA-C colocalization depends strictly on SMO activity state and ruling out potential nonspecific effects of SMO overexpression on SMO / PKA-C ciliary colocalization[35].

SMO / PKA-C colocalization occurred with somewhat slower kinetics than SMO phosphorylation but was nevertheless readily detectable by one hour of SAG treatment (Fig. 5A), consistent with SMO phosphorylation preceding PKA-C recruitment during this process. Critically, SAG-induced SMO / PKA-C colocalization in cilia was abolished by treatment with either Cmpd101 or 14as (Fig 5B, S5A). These studies demonstrate that GRK2 phosphorylation controls SMO / PKA-C interaction in cilia.

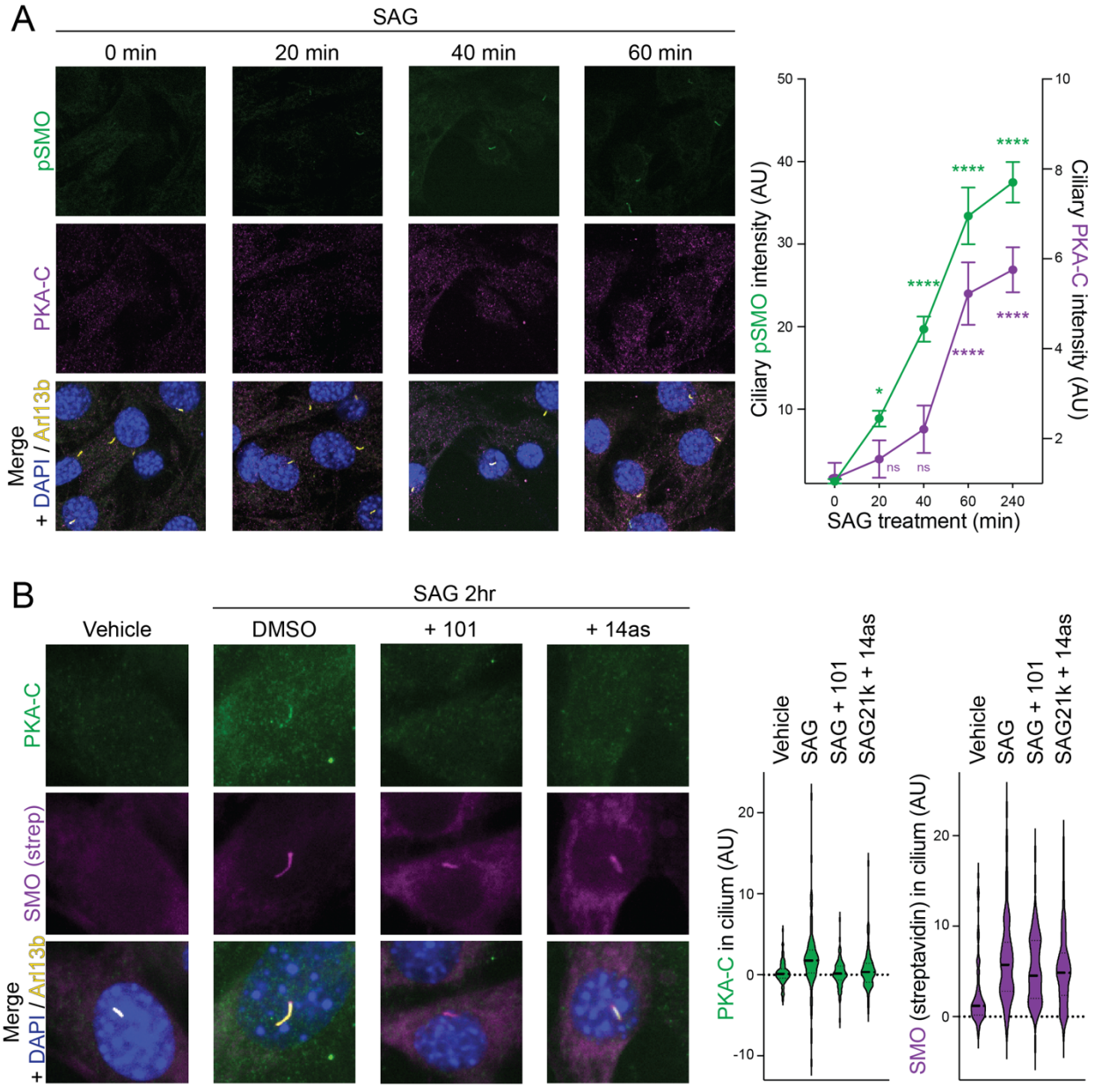

Figure 5: GRK2 phosphorylation is required for SMO / PKA-C interaction in the cilium.
(A) NIH3T3 cells stably expressing SMO-V5-TurboID were pretreated with cyclopamine for 16hr, followed by SAG for the indicated times, and accumulation of PKA-C (magenta) and phosphorylated SMO (pSMO, green) in cilia (Arl13b, yellow) were monitored via immunofluorescence microscopy. Left: raw data; Right: quantification of pSMO (left axis) and PKA-C (right axis).
(B) NIH3T3 cells stably expressing SMO-V5-TurboID were treated with SAG, either alone or in the presence of Cmpd101 or 14as for 2 hours, then subject to biotin treatment, fixed, and stained for PKA-C (green), streptavidin (magenta), Arl13b (yellow), and DAPI (blue). Streptavidin staining marks the localization of SMO-V5-TurboID in the cilium. Left: raw data; Right: quantification.

GRK2 phosphorylation of SMO is sufficient to induce SMO / PKA-C interaction

We next sought to uncover the biochemical mechanism by which GRK2 phosphorylation promotes formation of SMO / PKA-C complexes. We considered two possible models. Phosphorylation of SMO may trigger a direct interaction with PKA-C (Fig. 6A, "direct"). Alternatively, phosphorylation may recruit additional proteins that promote the SMO / PKA-C interaction (Fig. 6A, "indirect").

To distinguish between these scenarios, we biochemically reconstituted SMO / PKA-C complexes using purified proteins *in vitro*. Biochemical reconstitution is uniquely suited to address these models because it enables a stringent definition of the minimal set of factors required for GRK2 phosphorylation to enhance SMO / PKA-C interactions. In contrast, such questions are nearly impossible to address in the complex, biochemically undefined environments of cells or organisms, where proteins, lipids, metabolites, and other molecules or ions may contribute to interactions between GRK2-phosphorylated SMO and PKA-C.

Our strategy was to prepare purified SMO protein in GRK2-phosphorylated or non-phosphorylated states, and then evaluate the ability of each of these preparations to bind purified PKA-C *in vitro.* To obtain homogeneously phosphorylated SMO, we developed procedures to purify near-full-length SMO including the extracellular cysteine rich domain (CRD), 7TM domain, and pCT (Fig. S6A), then optimized conditions to phosphorylate SMO *in vitro* using purified GRK2 (see Methods). Following incubation with GRK2, we detected a strongly phosphorylated SMO species in the presence of SMO agonist but not SMO inverse agonist, manifest as incorporation of γ^{32}P-ATP in autoradiography (Fig S6B) and decreased electrophoretic mobility on SDS-PAGE (Fig 6B). These results are consistent with GRK2's preference for the SMO active conformation under physiological conditions[34,42] (Fig. 2). We confirmed via anti-pSMO immunoblotting that SMO underwent phosphorylation *in vitro* at the physiological GRK2 cluster (Fig. S6C). To prepare non-phosphorylated SMO, we expressed and purified SMO in the presence of an inverse agonist,

thereby avoiding phosphorylation by endogenous GRK2 in our HEK293 cell expression system, and omitted the *in vitro* GRK2 phosphorylation step.

We evaluated whether SMO phosphorylation is sufficient to enable binding to PKA-C using a FLAG pulldown assay in detergent micelles. We mixed phosphorylated or nonphosphorylated FLAG-tagged SMO (Fig. S6D) with PKA-C in a buffer containing SAG21k to maintain SMO in an active conformation and Mg/ATP to promote PKA-C pseudosubstrate interactions[35], followed by FLAG affinity chromatography. Only trace amounts of PKA-C were bound by non-phosphorylated SMO, similar to those pulled down by a negative control SMO construct lacking the entire cytoplasmic domain (SMOΔCT, Fig. 6C). This result is consistent with the relatively modest affinity of PKA-C for a soluble, nonphosphorylated SMO pCT construct in surface plasmon resonance studies (K_D = 752 nM)[35]. In contrast, phosphorylated SMO readily bound PKA-C (Fig. 6C). Thus, GRK2 phosphorylation of SMO can enhance SMO / PKA-C interactions with no other proteins present. We note that SMO binds substoichiometric amounts of PKA-C in this assay (25 +/- 6.8% PKA-C/SMO ratio, n = 4 independent experiments), suggesting that additional factors present in living systems may increase the efficiency of the direct interactions we observe *in vitro* (see Discussion). Nevertheless, our *in vitro* experiments indicate that such factors are not absolutely required, leading us to conclude that the effect of GRK2 phosphorylation on SMO / PKA-C interactions is likely direct (Fig 6A, “direct”).

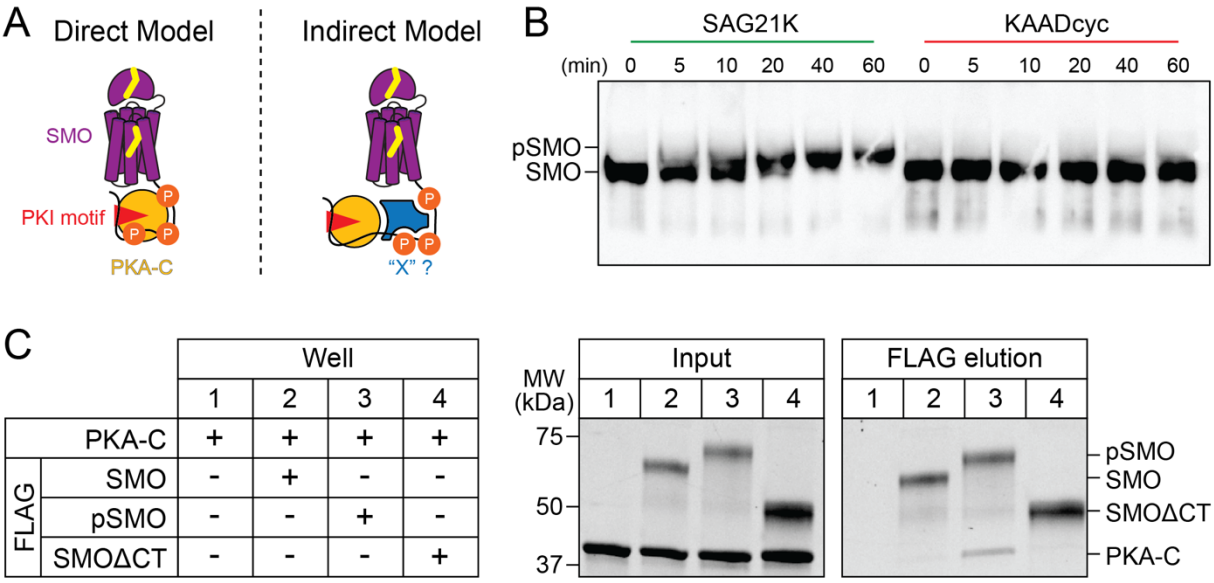

Figure 6: GRK2 phosphorylation of SMO is sufficient to induce SMO / PKA-C interaction
(A) Schematic diagram for two potential models of how GRK2 phosphorylation of SMO may promote interactions with PKA-C, either by directly triggering formation of a SMO / PKA-C complex ("Direct") or acting via an intermediary protein, symbolized as "X" ("Indirect"). See main text for additional information. **(B)** Purified FLAG-tagged SMO was subject to phosphorylation by GRK2 *in vitro* in the presence of SMO agonist (SAG21k) or inverse agonist (KAADcyc) for the indicated times (in min), and conversion of SMO to a phosphorylated form (pSMO) was analyzed by monitoring a mobility shift on SDS-PAGE via anti-FLAG immunoblotting. **(C)** Purified FLAG-tagged SMO in either a nonphosphorylated or phosphorylated state (SMO or pSMO, respectively), was mixed with PKA-C *in vitro* (10 μM each), and complex formation was detected via pulldown on anti-FLAG beads, followed by analysis of total protein in input and FLAG elution fractions on SDS-PAGE via Stain-free imaging. SMO lacking the cytoplasmic tail (FLAG-SMOΔCT) serves as a negative control for PKA-C binding. Position of SMO, pSMO, SMOΔCT, and PKA-C are indicated at right.

GRK2 phosphorylation of ciliary SMO is a general, evolutionarily conserved component of Hh signal transduction *in vivo*

Our findings thus far establish that the ciliary SMO-GRK2-PKA communication pathway operates in fibroblast cell lines, but whether this also occurs during Hh signal transduction in other biological contexts remains unknown. To address this knowledge gap, we utilized our anti-pSMO antibody, which readily detects phosphorylation of endogenous SMO via a highly conserved phospho-epitope (Fig. 2A), to ask whether SMO undergoes GRK2-mediated phosphorylation in a range of cellular and *in vivo* contexts. We focused primarily on the nervous system, where Hh signaling plays numerous well-established roles in proliferation and differentiation, both during embryogenesis and postnatally[62–64].

We first utilized the embryonic neural tube to study the instructive role of Hh signaling in cell fate decisions during neural development. This structure, the precursor to the spinal cord, is patterned by Sonic hedgehog (Shh) produced by the notochord and floor plate, which diffuses along the dorsal-ventral axis to form a gradient that instructs neuronal cell fate decisions in a concentration- and duration-dependent fashion[65,66]. When applied to neural tube sections from wild-type mice, the anti-pSMO antibody prominently stained cilia in the ventral neural tube, where levels of Shh are highest, but not in the dorsal neural tube where levels of Shh are low (Fig. 7A). The anti-pSMO stain was a faithful metric of SMO activation, as the signal observed in wild-type mice (Smo^{WT}) was noticeably weaker in a *Smo* hypomorphic mutant (Smo^{cbb}), considerably stronger in a *Smo* gain-of-function mutant that induces constitutive pathway activation (Smo^{M2}), and absent in a *Smo* null mutant (Smo^{bnb})[67–69] (Fig. 7A). To determine whether SMO is phosphorylated during neural development in other vertebrate species, we stained whole-mount zebrafish embryos (24 hours post-fertilization) with our anti-pSMO antibody. Again, we observed an intense anti-pSMO staining in cilia at the ventral but not the dorsal spinal cord, representing a population of neuronal progenitors that require high levels of Shh to generate primary motor

neurons (pMN) and oligodendrocytes[70–72] (Fig 7B). Thus, SMO undergoes activity-dependent GRK2 phosphorylation during instructive Hh signaling in vertebrate neural tube development.

We extended our analysis of SMO phosphorylation to the early zebrafish brain and eye field primordium, both of which are patterned by Shh produced at the embryonic midline[73–75]. Here we observed sparse but detectable ciliary anti-pSMO staining that was dramatically enhanced by treatment of embryos with SAG21k, demonstrating endogenous SMO phosphorylation in these structures and consistent with the ability of this SMO agonist to ectopically activate Hh signaling during embryogenesis (Fig S7B)[76–80]. Thus, SMO undergoes GRK2 phosphorylation during eye and brain development.

Lastly, we turned to the proliferation of mouse cerebellar granule neural precursors (CGNP) in culture as a model for mitogenic Hh signaling in the postnatal nervous system. Shortly after birth, Shh produced by the Purkinje cell layer of the cerebellum serves as the major mitogen for the adjacent CGNPs, driving Hh signal transduction that leads to transcription of genes involved in cell cycle entry and ultimately fueling a nearly one thousand-fold expansion of the cerebellum[81–84]. This phenomenon can be recapitulated in culture, where CGNPs dissected from postnatal mice and cultured *ex vivo* mount a robust proliferative response to Hh pathway stimulation that requires SMO activity and primary cilia. Primary CGNP cultures treated with SAG but not a vehicle control displayed strong ciliary anti-pSMO staining, demonstrating that GRK2 phosphorylates active SMO during CGNP proliferation (Fig 7C).

Taken together, our findings in mouse and zebrafish neural progenitors, zebrafish eye and forebrain precursor cells, and mouse CGNPs, all demonstrate that GRK2 phosphorylation of SMO is a general, evolutionarily conserved aspect of vertebrate Hh signal transduction.

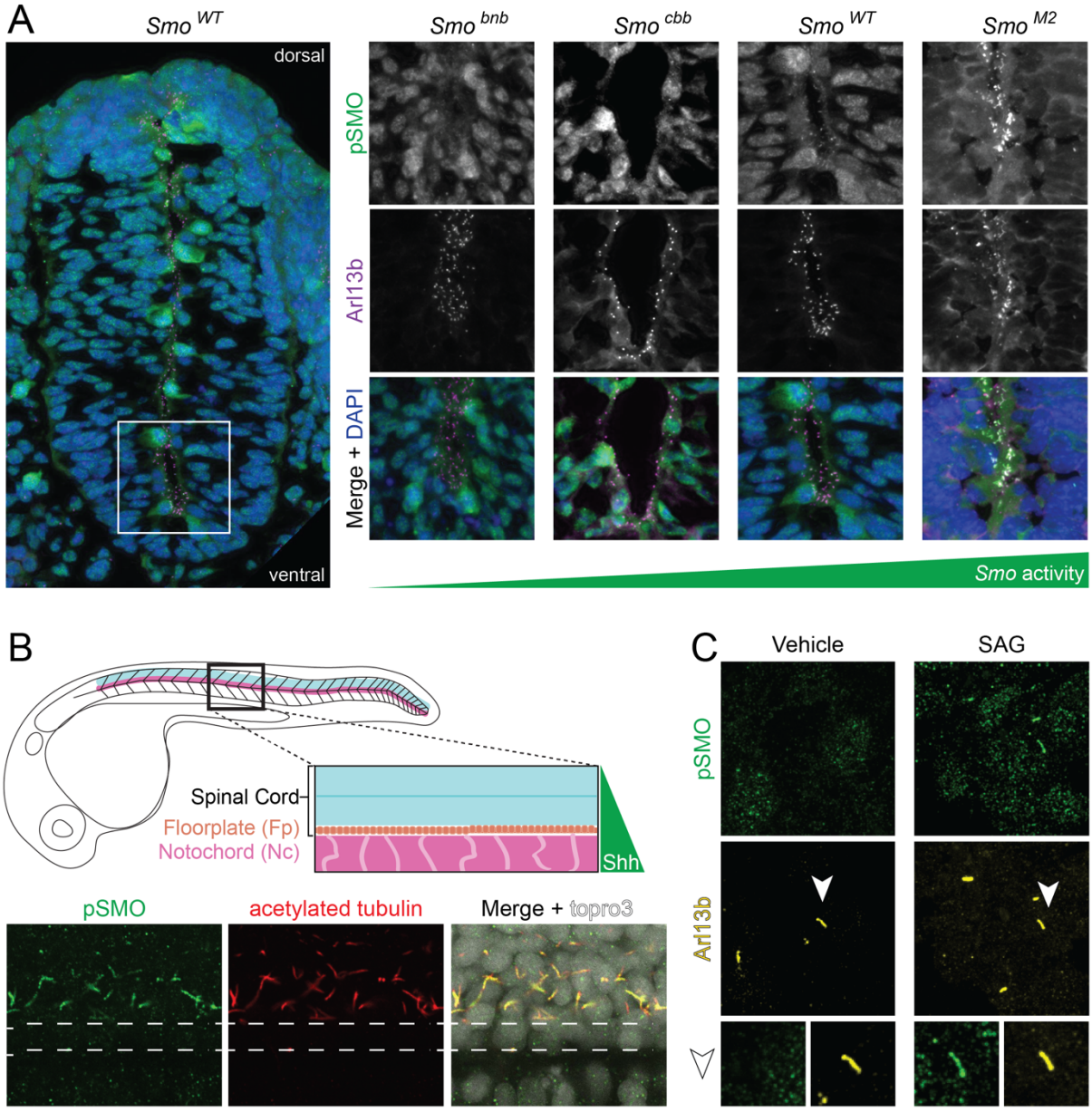

Figure 7: GRK2 phosphorylation of ciliary SMO is a general, evolutionarily conserved aspect of Hh signal transduction *in vivo*

(A) Neural tubes from the indicated wild-type or *Smo* mutant E9.5 mice (low-magnification view of wild-type mouse at left, higher-magnification view of wild-type or *Smo* alleles of differing strengths at right, see main text) were stained for pSMO and Arl13b. Images are oriented with dorsal pointing up and ventral pointing down. **(B)** Whole-mount zebrafish embryos at 24 hours post-fertilization (hpf) were stained with antibodies against pSMO (green) and cilia (acetylated tubulin, red), with topro3 counterstain to mark nuclei (gray). Close-up view of the ventral spinal cord is shown, with the dorsal spinal cord facing up and the ventral spinal cord facing down. **(C)** CGNPs freshly isolated from neonatal mice were cultured *ex vivo* and treated with vehicle (top) or SAG (bottom), followed by staining with anti-pSMO (green) and Arl13b (yellow).

DISCUSSION

SMO inhibition of PKA-C is fundamental to Hh signal transduction in development, homeostasis, and disease[2–4,30]. Here we define GRK2 as an indispensable regulator of this inhibition during Hh signal transduction in primary cilia. We show that ciliary GRK2 rapidly recognizes the active, agonist-bound conformation of SMO, and subsequently phosphorylates essential sites in the SMO pCT. This phosphorylation is: 1) sufficient to trigger direct SMO / PKA-C interactions, 2) required for SMO to engage PKA-C in cilia, and 3) a general feature of SMO activation by naturally occurring and synthetic SMO agonists, and in multiple cellular and *in vivo* contexts. Together with prior functional studies[34,35,39–41], our work establishes GRK2 phosphorylation of SMO, and the ensuing PKA-C recruitment and inactivation, as critical initiating events for the intracellular steps in Hh signal transduction. These findings provide a deeper understanding of canonical Hh signal transduction throughout development and disease. Furthermore, we anticipate that the tools and concepts established here will enable future cell biological investigations of SMO-GLI communication in many tissue, organ, and animal contexts.

Our work helps to resolve outstanding questions regarding whether SMO is a target of GRK2 kinases under physiological conditions[39,40,51,85]. Our previous studies implicating GRK2 in SMO / PKA-C signaling relied on reductionist experimental systems that do not fully reflect Hh signal transduction in its native ciliary context. Thus, while SMO undergoes activity-dependent phosphorylation by GRK2 in transfected HEK293 cells[34], whether this occurs during endogenous Hh signaling in primary cilia was merely inferred but never evaluated directly. In the present study, we addressed these issues by developing microscopy approaches to sensitively track GRK2 localization over time, as well as an anti-pSMO antibody to directly monitor phosphorylation of endogenous SMO in cilia. Using these approaches, we find that GRK2 recognizes and phosphorylates the active conformation of SMO in cilia. We also show that GRK2 activity is necessary for SMO to engage PKA-C in cilia, echoing the strong requirement for GRK2 during SMO-GLI communication[39–41]. Thus, the current study, together with prior mutagenesis and

pharmacology data, support a model in which GRK2 phosphorylates the SMO active conformation, enabling binding and inhibition of PKA-C during physiological Hh signal transduction in cilia.

Our study also provides new insights into the biochemical mechanism by which GRK2 phosphorylation promotes SMO / PKA-C interactions. We previously showed that GRK2 phosphorylation is necessary for SMO to bind PKA-C in cells[34], but it was not clear whether phosphorylation directly enhances SMO / PKA-C binding or whether the effect requires additional as-yet-unidentified proteins. We now establish using biochemical reconstitution that GRK2 phosphorylation can enhance binding of purified, near-full-length SMO to purified PKA-C *in vitro*. This result reveals that GRK2 phosphorylation is not merely a permissive event that facilitates the action of another protein on the SMO / PKA-C complex, but is sufficient on its own to trigger SMO / PKA-C binding. In contrast, if the effect of phosphorylation on the interaction needed additional factors, then phosphorylated SMO would not engage PKA-C more efficiently than would non-phosphorylated SMO in our experiments. We note, however, that proteins, lipids, or other factors not present in our *in vitro* system, while not absolutely required, may render phosphorylation-induced SMO / PKA-C binding more efficient in living systems, especially because SMO binds substoichiometric amounts of PKA-C in our *in vitro* assay. We expect such factors would play important roles in Hh signaling, and our *in vitro* biochemical system may enable their future discovery and characterization.

Based on our findings, we propose the following model for SMO-GRK2-PKA communication during Hh signal transduction (Fig. 8). In the Hh pathway "off" state, GRK2 is poised at the base of the cilium, but SMO is in an inactive conformation and cannot be recognized or phosphorylated by GRK2. As a result, PKA-C is active in the cilium (at the base and/or the shaft), and can phosphorylate and inactivate GLI[16,29,60,61] (Fig. 8, left panel). In the Hh pathway "on" state, SMO binds sterols and assumes an active conformation, triggering GRK2 to recognize active SMO, accumulate in the ciliary shaft, and phosphorylate the SMO pCT (Fig. 8, middle

panel). Consequently, SMO can bind and inhibit PKA-C in the ciliary shaft, leading to GLI activation (Fig. 8, right panel). These processes are further strengthened by the accumulation of SMO protein to high levels in the cilium over the course of several hours following SMO activation[27,28], which serves as a positive feedback loop for SMO-GRK2-PKA communication pathway described above. Our prior experiments in cultured fibroblasts and zebrafish embryos support an essential role for the SMO-GRK2-PKA communication pathway in Hh signal transduction[34,35], but SMO can also affect ciliary PKA via at least two additional routes: 1) coupling to inhibitory G proteins ($G\alpha_i$)[86–88], which block PKA-C via classical cAMP-dependent pathways; 2) stimulating the ciliary exit of GPR161, a constitutively active GPCR that activates PKA-C by coupling to stimulatory ($G\alpha_s$) G proteins[40,89–92]. Although these processes are not absolutely required for SMO-GLI communication[93–95], they likely make important, context-dependent contributions to GLI activation, as evidenced by the moderate Hh pathway overactivation observed in *Gpr161*$^{-/-}$ cells and embryos under certain conditions[40,89–91]. In sum, the SMO-GRK2-PKA regulatory mechanism, operating in concert with other SMO-PKA signaling pathways, ensures that only the active state of SMO can bind and inhibit PKA-C in the cilium, and thereby helps to avoid pathologic outcomes associated with too much or too little GLI activation[14].

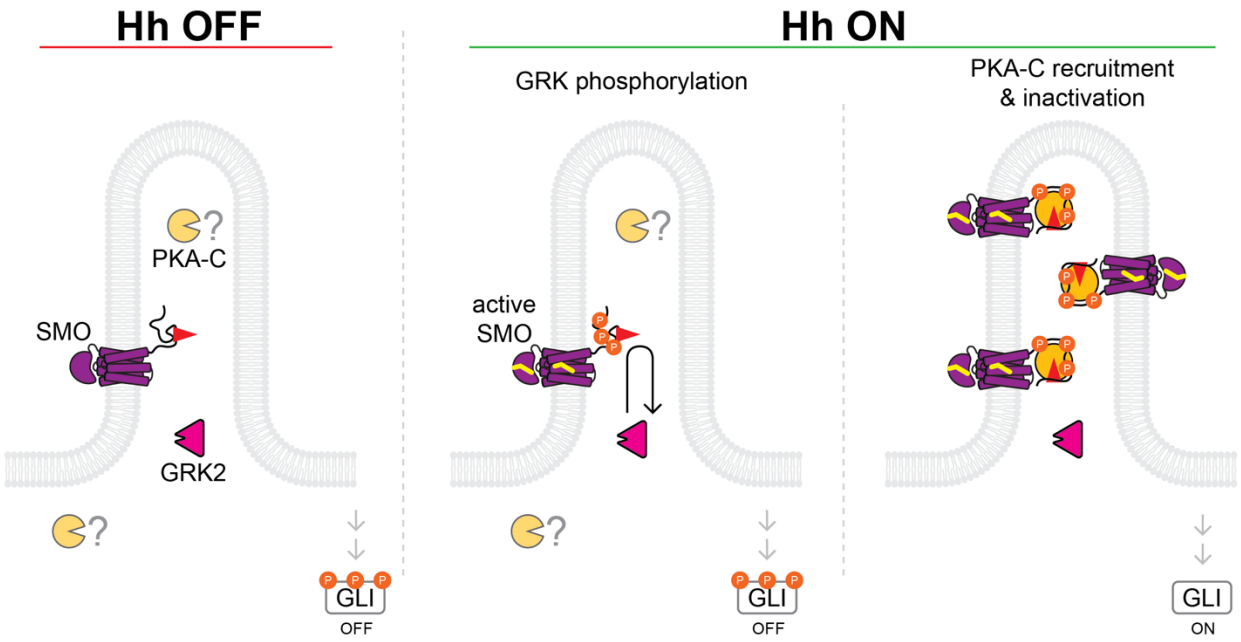

Figure 8: Model for SMO-GRK2-PKA communication during Hh signal transduction. See main text for details.

An outstanding challenge is to understand in structural terms how GRK2 recognizes and phosphorylates the SMO active conformation. Some clues may be provided by recent cryoEM structures of GRK1 in complex with the GPCR rhodopsin[38,96]. In these studies, GRK1 recognizes the active conformation of rhodopsin by inserting its N-terminal α-helix (αN) into an intracellular rhodopsin cavity exposed by outward movement of TM helices 5 and 6 during rhodopsin activation. This docking event activates GRK1, enabling phosphorylation of rhodopsin intracellular domains, followed by dissociation of the rhodopsin-GRK1 complex. We speculate that a similar process underlies GRK2 recognition and phosphorylation of active SMO, as SMO activation causes an outward shift in TM helices 5 and 6[23], and GRK2 harboring point mutations in the αN helix fail to rescue the loss of SMO-GLI communication observed in $Grk2^{-/-}$ cells[40]. Nevertheless, other regions of GRK2 critical for GPCR regulation, such as the phosphoinositide- and Gβγ-binding pleckstrin homology domain[36,37], are not conserved in GRK1[38,96], and the structural basis for these regions to enable GRK2 phosphorylation of SMO and other GPCRs is presently unclear. The structural mechanism by which phosphorylation enhances binding of PKA-C to SMO is also mysterious, as SMO is, to our knowledge, the first example of a PKA-C decoy substrate whose binding is regulated by phosphorylation[97–99]. Future structural studies of SMO-GRK complexes, as well as complexes between phosphorylated SMO and PKA-C, will help to address these questions.

We observed that SMO phosphorylation by GRK2, although occurring almost immediately after SMO activation, also depends on continuous action of these kinases, as treatment with a GRK2 inhibitor triggers disappearance of phosphorylated SMO within minutes. The mechanisms underlying this rapid disappearance are currently unknown. Levels of SMO remain constant in these experiments, ruling out effects of phosphorylation on SMO stability. The rapid kinetics hint that one or more cellular phosphatases[100,101] may dephosphorylate SMO, either tonically or in response to SMO activation, thereby counterbalancing the effect of GRK2. Such a mechanism

may serve to adjust steady-state SMO phosphorylation levels, potentially impacting the timing and intensity of SMO-GLI communication during Hh signal transduction. Future studies can evaluate these hypotheses by identifying candidate phosphatases that act on SMO and delineating their underlying modes of regulation. Our studies also reveal that PKA-C colocalizes with phosphorylated SMO, but with somewhat slower kinetics than those of SMO phosphorylation. Although these findings are consistent with SMO phosphorylation preceding and triggering PKA-C interaction, the cell biological basis for the observed delay in PKA-C interaction remains unclear. It is possible that this reflects a technical limitation, in that SMO phosphorylation may be easier to detect than PKA-C ciliary accumulation. Alternatively, PKA-C might not gain access to SMO in cilia via simple diffusion, but rather might be titrated via a regulated trafficking process that dictates the timing and extent of PKA-C ciliary localization. Such a mechanism would likely influence Hh along with other PKA-dependent ciliary pathways and may be revealed by more detailed studies of PKA-C ciliary trafficking mechanisms.

Beyond SMO and GRK2 in the Hh pathway, our study also has general implications for other ciliary GPCRs and GRKs. Our work provides the first direct demonstration that a GRK can localize in or near the cilium, and that a ciliary GPCR undergoes GRK-mediated phosphorylation. It seems unlikely, however, that the pool of GRK2 at the base of the cilium is singularly dedicated to serving the needs of SMO during Hh signal transduction. Indeed, the cilium is home to a host of GPCRs critical to the nervous, cardiovascular, and musculoskeletal systems, and dysregulation of these receptors is associated with a range of devastating pathologies[9,10,102]. Many of these GPCRs are assumed to undergo agonist-dependent GRK phosphorylation in the cilium, but to our knowledge this has never been demonstrated directly. We expect that the concepts and approaches developed here will enable studies of GRK ciliary localization as well as phosphorylation of ciliary GPCRs and the ensuing downstream signaling processes. Such studies will enable a better understanding of how GPCRs signal within cilia and how dysregulation of

these processes instigates disease. GRK phosphorylation of GPCRs is canonically associated with β-arrestin binding[31,32,37,38]. In contrast, our studies reveal a new type of role for GRKs, in which receptor phosphorylation triggers direct interactions with PKA-C. This finding suggests that GRK phosphorylation may enable activated GPCRs to directly bind a variety of intracellular signaling factors, including β-arrestin, PKA-C, and perhaps other proteins as well. Such mechanisms may enable GPCR activation to encode a broad range of signaling outputs and thereby produce a wide array of biological outcomes. Given the emerging examples of direct GPCR coupling to factors other than heterotrimeric G proteins and β-arrestins[103–106], understanding these signaling mechanisms may provide an exciting research direction in the coming years.

ACKNOWLEDGMENTS

We thank J. Reiter, K. Hilgendorf, M. Nachury, and S. Nakielny for providing feedback on our manuscript. This work was supported by and Ellison Foundation Research Scholar Grant from the American Cancer Society (R.S.), an NSF CAREER award (IOS- 2143711) (X.G.) and the National Institutes of Health grant numbers R01 HL071818 (J.J.G.T.), 1R01GM145651 (R.S.), 1R15CA235749-01 (X.G.), 5R01GM143276-02 (X.G.), and 1R35GM133672 (B.R.M.).

COMPETING FINANCIAL INTERESTS

S.S. is the founder and scientific advisor of 7TM Antibodies GmbH, Jena, Germany. F.N. is an employee of 7TM Antibodies. All other authors declare no competing interests.

SUPPLEMENTARY MOVIES

Supplementary Movie 1. Live-cilium TIRF movie of IMCD3 cells stably expressing GRK2-eGFP, with images acquired at 3 minute intervals. Cells are pre-imaged for 15 min, and SAG21k is added at the 0 min timepoint, followed by continued monitoring (see Main text.) Labels and colors are

as in Fig 1. The SirTubulin (red) and GRK2-eGFP (gray) channels are shifted laterally with respect to one another, to facilitate viewing.

REFERENCES

1. Briscoe, J., and Thérond, P.P. (2013). The mechanisms of Hedgehog signalling and its roles in development and disease. Nat. Rev. Mol. Cell Biol. *14*, 416–429.

2. Ingham, P.W. (2022). Hedgehog signaling. Curr. Top. Dev. Biol. *149*, 1–58.

3. Kong, J.H., Siebold, C., and Rohatgi, R. (2019). Biochemical mechanisms of vertebrate hedgehog signaling. Development *146*. 10.1242/dev.166892.

4. Zhang, Y., and Beachy, P.A. (2023). Cellular and molecular mechanisms of Hedgehog signalling. Nat. Rev. Mol. Cell Biol. 10.1038/s41580-023-00591-1.

5. Pak, E., and Segal, R.A. (2016). Hedgehog Signal Transduction: Key Players, Oncogenic Drivers, and Cancer Therapy. Dev. Cell *38*, 333–344.

6. Wu, F., Zhang, Y., Sun, B., McMahon, A.P., and Wang, Y. (2017). Hedgehog Signaling: From Basic Biology to Cancer Therapy. Cell Chem Biol *24*, 252–280.

7. Gigante, E.D., and Caspary, T. (2020). Signaling in the primary cilium through the lens of the Hedgehog pathway. Wiley Interdiscip. Rev. Dev. Biol. *9*, e377.

8. Goetz, S.C., and Anderson, K.V. (2010). The primary cilium: a signalling centre during vertebrate development. Nat. Rev. Genet. *11*, 331–344.

9. Reiter, J.F., and Leroux, M.R. (2017). Genes and molecular pathways underpinning ciliopathies. Nat. Rev. Mol. Cell Biol. *18*, 533–547.

10. Mill, P., Christensen, S.T., and Pedersen, L.B. (2023). Primary cilia as dynamic and diverse signalling hubs in development and disease. Nat. Rev. Genet. 10.1038/s41576-023-00587-9.

11. Lv, B., Stuck, M.W., Desai, P.B., Cabrera, O.A., and Pazour, G.J. (2021). E3 ubiquitin ligase Wwp1 regulates ciliary dynamics of the Hedgehog receptor Smoothened. J. Cell Biol. *220*. 10.1083/jcb.202010177.

12. Desai, P.B., Stuck, M.W., Lv, B., and Pazour, G.J. (2020). Ubiquitin links smoothened to intraflagellar transport to regulate Hedgehog signaling. J. Cell Biol. *219*. 10.1083/jcb.201912104.

13. Shinde, S.R., Nager, A.R., and Nachury, M.V. (2020). Ubiquitin chains earmark GPCRs for BBSome-mediated removal from cilia. J. Cell Biol. *219*. 10.1083/jcb.202003020.

14. Hui, C.-C., and Angers, S. (2011). Gli proteins in development and disease. Annu. Rev. Cell Dev. Biol. *27*, 513–537.

15. Hammerschmidt, M., Bitgood, M.J., and McMahon, A.P. (1996). Protein kinase A is a common negative regulator of Hedgehog signaling in the vertebrate embryo. Genes Dev. *10*, 647–658.

16. Tuson, M., He, M., and Anderson, K.V. (2011). Protein kinase A acts at the basal body of the primary cilium to prevent Gli2 activation and ventralization of the mouse neural tube. Development *138*, 4921–4930.

17. Aza-Blanc, P., Ramírez-Weber, F.A., Laget, M.P., Schwartz, C., and Kornberg, T.B. (1997). Proteolysis that is inhibited by hedgehog targets Cubitus interruptus protein to the nucleus and converts it to a repressor. Cell *89*, 1043–1053.

18. Humke, E.W., Dorn, K.V., Milenkovic, L., Scott, M.P., and Rohatgi, R. (2010). The output of Hedgehog signaling is controlled by the dynamic association between Suppressor of Fused and the Gli proteins. Genes Dev. *24*, 670–682.

19. Méthot, N., and Basler, K. (1999). Hedgehog controls limb development by regulating the activities of distinct transcriptional activator and repressor forms of Cubitus interruptus. Cell *96*, 819–831.

20. Niewiadomski, P., Kong, J.H., Ahrends, R., Ma, Y., Humke, E.W., Khan, S., Teruel, M.N., Novitch, B.G., and Rohatgi, R. (2014). Gli protein activity is controlled by multisite phosphorylation in vertebrate Hedgehog signaling. Cell Rep. *6*, 168–181.

21. Wang, B., Fallon, J.F., and Beachy, P.A. (2000). Hedgehog-regulated processing of Gli3 produces an anterior/posterior repressor gradient in the developing vertebrate limb. Cell *100*, 423–434.

22. Byrne, E.F.X., Sircar, R., Miller, P.S., Hedger, G., Luchetti, G., Nachtergaele, S., Tully, M.D., Mydock-McGrane, L., Covey, D.F., Rambo, R.P., et al. (2016). Structural basis of Smoothened regulation by its extracellular domains. Nature *535*, 517–522.

23. Deshpande, I., Liang, J., Hedeen, D., Roberts, K.J., Zhang, Y., Ha, B., Latorraca, N.R., Faust, B., Dror, R.O., Beachy, P.A., et al. (2019). Smoothened stimulation by membrane sterols drives Hedgehog pathway activity. Nature *571*, 284–288.

24. Qi, X., Friedberg, L., De Bose-Boyd, R., Long, T., and Li, X. (2020). Sterols in an intramolecular channel of Smoothened mediate Hedgehog signaling. Nat. Chem. Biol. *16*, 1368–1375.

25. Huang, P., Zheng, S., Wierbowski, B.M., Kim, Y., Nedelcu, D., Aravena, L., Liu, J., Kruse, A.C., and Salic, A. (2018). Structural basis of smoothened activation in hedgehog signaling. Cell *174*, 312-324.e16.

26. Corbit, K.C., Aanstad, P., Singla, V., Norman, A.R., Stainier, D.Y.R., and Reiter, J.F. (2005). Vertebrate Smoothened functions at the primary cilium. Nature *437*, 1018–1021.

27. Rohatgi, R., Milenkovic, L., and Scott, M.P. (2007). Patched1 regulates hedgehog signaling at the primary cilium. Science *317*, 372–376.

28. Kim, J., Kato, M., and Beachy, P.A. (2009). Gli2 trafficking links Hedgehog-dependent activation of Smoothened in the primary cilium to transcriptional activation in the nucleus. Proc. Natl. Acad. Sci. U. S. A. *106*, 21666–21671.

29. Li, J., Wang, C., Wu, C., Cao, T., Xu, G., Meng, Q., and Wang, B. (2017). PKA-mediated Gli2 and Gli3 phosphorylation is inhibited by Hedgehog signaling in cilia and reduced in Talpid3 mutant. Dev. Biol. *429*, 147–157.

30. Cai, E., Zhang, J., and Ge, X. (2021). Control of the Hedgehog pathway by compartmentalized PKA in the primary cilium. Sci. China Life Sci. 10.1007/s11427-021-1975-9.

31. Lefkowitz, R.J. (2000). The superfamily of heptahelical receptors. Nat. Cell Biol. *2*, E133-6.

32. Pierce, K.L., Premont, R.T., and Lefkowitz, R.J. (2002). Seven-transmembrane receptors. Nat. Rev. Mol. Cell Biol. *3*, 639–650.

33. Ayers, K.L., and Thérond, P.P. (2010). Evaluating Smoothened as a G-protein-coupled receptor for Hedgehog signalling. Trends Cell Biol. *20*, 287–298.

34. Arveseth, C.D., Happ, J.T., Hedeen, D.S., Zhu, J.-F., Capener, J.L., Klatt Shaw, D., Deshpande, I., Liang, J., Xu, J., Stubben, S.L., et al. (2021). Smoothened transduces Hedgehog signals via activity-dependent sequestration of PKA catalytic subunits. PLoS Biol. *19*, e3001191.

35. Happ, J.T., Arveseth, C.D., Bruystens, J., Bertinetti, D., Nelson, I.B., Olivieri, C., Zhang, J., Hedeen, D.S., Zhu, J.-F., Capener, J.L., et al. (2022). A PKA inhibitor motif within SMOOTHENED controls Hedgehog signal transduction. Nat. Struct. Mol. Biol. *29*, 990–999.

36. Gurevich, E.V., Tesmer, J.J.G., Mushegian, A., and Gurevich, V.V. (2012). G protein-coupled receptor kinases: more than just kinases and not only for GPCRs. Pharmacol. Ther. *133*, 40–69.

37. Komolov, K.E., and Benovic, J.L. (2018). G protein-coupled receptor kinases: Past, present and future. Cell. Signal. *41*, 17–24.

38. Chen, Q., and Tesmer, J.J.G. (2022). G protein-coupled receptor interactions with arrestins and GPCR kinases: The unresolved issue of signal bias. J. Biol. Chem. *298*, 102279.

39. Zhao, Z., Lee, R.T.H., Pusapati, G.V., Iyu, A., Rohatgi, R., and Ingham, P.W. (2016). An essential role for Grk2 in Hedgehog signalling downstream of Smoothened. EMBO Rep. *17*, 739–752.

40. Pusapati, G.V., Kong, J.H., Patel, B.B., Gouti, M., Sagner, A., Sircar, R., Luchetti, G., Ingham, P.W., Briscoe, J., and Rohatgi, R. (2018). G protein-coupled receptors control the sensitivity of cells to the morphogen Sonic Hedgehog. Sci. Signal. *11*. 10.1126/scisignal.aao5749.

41. Bosakova, M., Abraham, S.P., Nita, A., Hruba, E., Buchtova, M., Taylor, S.P., Duran, I., Martin, J., Svozilova, K., Barta, T., et al. (2020). Mutations in GRK2 cause Jeune syndrome by impairing Hedgehog and canonical Wnt signaling. EMBO Mol. Med. *12*, e11739.

42. Chen, W., Ren, X.-R., Nelson, C.D., Barak, L.S., Chen, J.K., Beachy, P.A., de Sauvage, F., and Lefkowitz, R.J. (2004). Activity-dependent internalization of smoothened mediated by beta-arrestin 2 and GRK2. Science *306*, 2257–2260.

43. Haycraft, C.J., Banizs, B., Aydin-Son, Y., Zhang, Q., Michaud, E.J., and Yoder, B.K. (2005). Gli2 and Gli3 localize to cilia and require the intraflagellar transport protein polaris for processing and function. PLoS Genet. *1*, e53.

44. Stoeber, M., Jullié, D., Li, J., Chakraborty, S., Majumdar, S., Lambert, N.A., Manglik, A., and von Zastrow, M. (2020). Agonist-selective recruitment of engineered protein probes and of GRK2 by opioid receptors in living cells. Elife *9*. 10.7554/eLife.54208.

45. Radoux-Mergault, A., Oberhauser, L., Aureli, S., Gervasio, F.L., and Stoeber, M. (2023). Subcellular location defines GPCR signal transduction. Sci Adv *9*, eadf6059.

46. May, E.A., Kalocsay, M., D'Auriac, I.G., Schuster, P.S., Gygi, S.P., Nachury, M.V., and Mick, D.U. (2021). Time-resolved proteomics profiling of the ciliary Hedgehog response. J. Cell Biol. *220*. 10.1083/jcb.202007207.

47. Pal, K., Hwang, S.-H., Somatilaka, B., Badgandi, H., Jackson, P.K., DeFea, K., and Mukhopadhyay, S. (2016). Smoothened determines β-arrestin-mediated removal of the G protein-coupled receptor Gpr161 from the primary cilium. J. Cell Biol. *212*, 861–875.

48. Taipale, J., Chen, J.K., Cooper, M.K., Wang, B., Mann, R.K., Milenkovic, L., Scott, M.P., and Beachy, P.A. (2000). Effects of oncogenic mutations in Smoothened and Patched can be reversed by cyclopamine. Nature *406*, 1005–1009.

49. Myers, B.R., Sever, N., Chong, Y.C., Kim, J., Belani, J.D., Rychnovsky, S., Bazan, J.F., and Beachy, P.A. (2013). Hedgehog pathway modulation by multiple lipid binding sites on the smoothened effector of signal response. Dev. Cell *26*, 346–357.

50. Waldschmidt, H.V., Homan, K.T., Cato, M.C., Cruz-Rodríguez, O., Cannavo, A., Wilson, M.W., Song, J., Cheung, J.Y., Koch, W.J., Tesmer, J.J.G., et al. (2017). Structure-Based Design of Highly Selective and Potent G Protein-Coupled Receptor Kinase 2 Inhibitors Based on Paroxetine. J. Med. Chem. *60*, 3052–3069.

51. Chen, Y., Sasai, N., Ma, G., Yue, T., Jia, J., Briscoe, J., and Jiang, J. (2011). Sonic Hedgehog dependent phosphorylation by CK1α and GRK2 is required for ciliary accumulation and activation of smoothened. PLoS Biol. *9*, e1001083.

52. Li, S., Li, S., Han, Y., Tong, C., Wang, B., Chen, Y., and Jiang, J. (2016). Regulation of Smoothened Phosphorylation and High-Level Hedgehog Signaling Activity by a Plasma Membrane Associated Kinase. PLoS Biol. *14*, e1002481.

53. Bain, J., Plater, L., Elliott, M., Shpiro, N., Hastie, C.J., McLauchlan, H., Klevernic, I., Arthur, J.S.C., Alessi, D.R., and Cohen, P. (2007). The selectivity of protein kinase inhibitors: a further update. Biochem. J. *408*, 297–315.

54. Rena, G., Bain, J., Elliott, M., and Cohen, P. (2004). D4476, a cell-permeant inhibitor of CK1, suppresses the site-specific phosphorylation and nuclear exclusion of FOXO1a. EMBO Rep. *5*, 60–65.

55. Zhang, F., Virshup, D.M., and Cheong, J.K. (2018). Oncogenic RAS-induced CK1α drives nuclear FOXO proteolysis. Oncogene *37*, 363–376.

56. Ocbina, P.J.R., and Anderson, K.V. (2008). Intraflagellar transport, cilia, and mammalian Hedgehog signaling: analysis in mouse embryonic fibroblasts. Dev. Dyn. *237*, 2030–2038.

57. Rohatgi, R., Milenkovic, L., Corcoran, R.B., and Scott, M.P. (2009). Hedgehog signal transduction by Smoothened: pharmacologic evidence for a 2-step activation process. Proc. Natl. Acad. Sci. U. S. A. *106*, 3196–3201.

58. Wilson, C.W., Chen, M.-H., and Chuang, P.-T. (2009). Smoothened adopts multiple active and inactive conformations capable of trafficking to the primary cilium. PLoS One *4*, e5182.

59. Tukachinsky, H., Petrov, K., Watanabe, M., and Salic, A. (2016). Mechanism of inhibition of the tumor suppressor Patched by Sonic Hedgehog. Proc. Natl. Acad. Sci. U. S. A. *113*, E5866–E5875.

60. Mick, D.U., Rodrigues, R.B., Leib, R.D., Adams, C.M., Chien, A.S., Gygi, S.P., and Nachury, M.V. (2015). Proteomics of Primary Cilia by Proximity Labeling. Dev. Cell *35*, 497–512.

61. Truong, M.E., Bilekova, S., Choksi, S.P., Li, W., Bugaj, L.J., Xu, K., and Reiter, J.F. (2021). Vertebrate cells differentially interpret ciliary and extraciliary cAMP. Cell *184*, 2911-2926.e18.

62. Hébert, J.M., and Fishell, G. (2008). The genetics of early telencephalon patterning: some assembly required. Nat. Rev. Neurosci. *9*, 678–685.

63. Yang, C., Qi, Y., and Sun, Z. (2021). The role of Sonic hedgehog pathway in the development of the central nervous system and aging-related neurodegenerative diseases. Front. Mol. Biosci. *8*, 711710.

64. Fuccillo, M., Joyner, A.L., and Fishell, G. (2006). Morphogen to mitogen: the multiple roles of hedgehog signalling in vertebrate neural development. Nat. Rev. Neurosci. *7*, 772–783.

65. Ribes, V., and Briscoe, J. (2009). Establishing and interpreting graded Sonic Hedgehog signaling during vertebrate neural tube patterning: the role of negative feedback. Cold Spring Harb. Perspect. Biol. *1*, a002014.

66. Jessell, T.M. (2000). Neuronal specification in the spinal cord: inductive signals and transcriptional codes. Nat. Rev. Genet. *1*, 20–29.

67. Kasarskis, A., Manova, K., and Anderson, K.V. (1998). A phenotype-based screen for embryonic lethal mutations in the mouse. Proc. Natl. Acad. Sci. U. S. A. *95*, 7485–7490.

68. Gigante, E.D., Long, A.B., Ben-Ami, J., and Caspary, T. (2018). Hypomorphic Smo mutant with inefficient ciliary enrichment disrupts the highest level of vertebrate Hedgehog response. Dev. Biol. *437*, 152–162.

69. Jeong, J., Mao, J., Tenzen, T., Kottmann, A.H., and McMahon, A.P. (2004). Hedgehog signaling in the neural crest cells regulates the patterning and growth of facial primordia. Genes Dev. *18*, 937–951.

70. Kearns, C.A., Walker, M., Ravanelli, A.M., Scott, K., Arzbecker, M.R., and Appel, B. (2021). Zebrafish spinal cord oligodendrocyte formation requires boc function. Genetics *218*. 10.1093/genetics/iyab082.

71. Ravanelli, A.M., Kearns, C.A., Powers, R.K., Wang, Y., Hines, J.H., Donaldson, M.J., and Appel, B. (2018). Sequential specification of oligodendrocyte lineage cells by distinct levels of Hedgehog and Notch signaling. Dev. Biol. *444*, 93–106.

72. Huang, P., Xiong, F., Megason, S.G., and Schier, A.F. (2012). Attenuation of Notch and Hedgehog signaling is required for fate specification in the spinal cord. PLoS Genet. *8*, e1002762.

73. Stenkamp, D.L. (2008). Multiple roles for hedgehog signalling in zebrafish eye development. In Shh and Gli Signalling and Development (Springer New York), pp. 58–68.

74. Amato, M.A., Boy, S., and Perron, M. (2004). Hedgehog signaling in vertebrate eye development: a growing puzzle. Cell. Mol. Life Sci. *61*, 899–910.

75. Casey, M.A., Lusk, S., and Kwan, K.M. (2021). Build me up optic cup: Intrinsic and extrinsic mechanisms of vertebrate eye morphogenesis. Dev. Biol. *476*, 128–136.

76. Li, X., Yang, S., Chinipardaz, Z., Koyama, E., and Yang, S. (2021). SAG therapy restores bone growth and reduces enchondroma incidence in a model of skeletal chondrodysplasias caused by Ihh deficiency. Mol. Ther. Methods Clin. Dev. *23*, 461–475.

77. Shin, J.-O., Song, J., Choi, H.S., Lee, J., Lee, K., Ko, H.W., and Bok, J. (2019). Activation of sonic hedgehog signaling by a Smoothened agonist restores congenital defects in mouse models of endocrine-cerebro-osteodysplasia syndrome. EBioMedicine *49*, 305–317.

78. Heine, V.M., Griveau, A., Chapin, C., Ballard, P.L., Chen, J.K., and Rowitch, D.H. (2011). A small-molecule smoothened agonist prevents glucocorticoid-induced neonatal cerebellar injury. Sci. Transl. Med. *3*, 105ra104.

79. Bragina, O., Sergejeva, S., Serg, M., Zarkovsky, T., Maloverjan, A., Kogerman, P., and Zarkovsky, A. (2010). Smoothened agonist augments proliferation and survival of neural cells. Neurosci. Lett. *482*, 81–85.

80. Delmotte, Q., Diabira, D., Belaidouni, Y., Hamze, M., Kochmann, M., Montheil, A., Gaiarsa, J.-L., Porcher, C., and Belgacem, Y.H. (2020). Sonic hedgehog signaling agonist (SAG) triggers BDNF secretion and promotes the maturation of GABAergic networks in the postnatal rat hippocampus. Front. Cell. Neurosci. *14*, 98.

81. Wechsler-Reya, R.J., and Scott, M.P. (1999). Control of neuronal precursor proliferation in the cerebellum by Sonic Hedgehog. Neuron *22*, 103–114.

82. Wallace, V.A. (1999). Purkinje-cell-derived Sonic hedgehog regulates granule neuron precursor cell proliferation in the developing mouse cerebellum. Curr. Biol. *9*, 445–448.

83. Barzi, M., Kostrz, D., Menendez, A., and Pons, S. (2011). Sonic Hedgehog-induced proliferation requires specific Gα inhibitory proteins. J. Biol. Chem. *286*, 8067–8074.

84. Barzi, M., Berenguer, J., Menendez, A., Alvarez-Rodriguez, R., and Pons, S. (2010). Sonic-hedgehog-mediated proliferation requires the localization of PKA to the cilium base. J. Cell Sci. *123*, 62–69.

85. Sharpe, H.J., and de Sauvage, F.J. (2018). Grking the Smoothened signal. Sci. Signal. *11*. 10.1126/scisignal.aar6377.

86. Shen, F., Cheng, L., Douglas, A.E., Riobo, N.A., and Manning, D.R. (2013). Smoothened is a fully competent activator of the heterotrimeric G protein G(i). Mol. Pharmacol. *83*, 691–697.

87. Riobo, N.A., Saucy, B., Dilizio, C., and Manning, D.R. (2006). Activation of heterotrimeric G proteins by Smoothened. Proc. Natl. Acad. Sci. U. S. A. *103*, 12607–12612.

88. Myers, B.R., Neahring, L., Zhang, Y., Roberts, K.J., and Beachy, P.A. (2017). Rapid, direct activity assays for Smoothened reveal Hedgehog pathway regulation by membrane cholesterol and extracellular sodium. Proc. Natl. Acad. Sci. U. S. A. *114*, E11141–E11150.

89. Mukhopadhyay, S., Wen, X., Ratti, N., Loktev, A., Rangell, L., Scales, S.J., and Jackson, P.K. (2013). The ciliary G-protein-coupled receptor Gpr161 negatively regulates the Sonic hedgehog pathway via cAMP signaling. Cell *152*, 210–223.

90. Shimada, I.S., Somatilaka, B.N., Hwang, S.-H., Anderson, A.G., Shelton, J.M., Rajaram, V., Konopka, G., and Mukhopadhyay, S. (2019). Derepression of sonic hedgehog signaling upon Gpr161 deletion unravels forebrain and ventricular abnormalities. Dev. Biol. *450*, 47–62.

91. Shimada, I.S., Hwang, S.-H., Somatilaka, B.N., Wang, X., Skowron, P., Kim, J., Kim, M., Shelton, J.M., Rajaram, V., Xuan, Z., et al. (2018). Basal suppression of the sonic hedgehog pathway by the G-protein-coupled receptor Gpr161 restricts medulloblastoma pathogenesis. Cell Rep. *22*, 1169–1184.

92. Tschaikner, P.M., Regele, D., Röck, R., Salvenmoser, W., Meyer, D., Bouvier, M., Geley, S., Stefan, E., and Aanstad, P. (2021). Feedback control of the Gpr161-Gαs-PKA axis contributes to basal Hedgehog repression in zebrafish. Development *148*. 10.1242/dev.192443.

93. Low, W.-C., Wang, C., Pan, Y., Huang, X.-Y., Chen, J.K., and Wang, B. (2008). The decoupling of Smoothened from Galphai proteins has little effect on Gli3 protein processing and Hedgehog-regulated chick neural tube patterning. Dev. Biol. *321*, 188–196.

94. Regard, J.B., Malhotra, D., Gvozdenovic-Jeremic, J., Josey, M., Chen, M., Weinstein, L.S., Lu, J., Shore, E.M., Kaplan, F.S., and Yang, Y. (2013). Activation of Hedgehog signaling by loss of GNAS causes heterotopic ossification. Nat. Med. *19*, 1505–1512.

95. Moore, B.S., Stepanchick, A.N., Tewson, P.H., Hartle, C.M., Zhang, J., Quinn, A.M., Hughes, T.E., and Mirshahi, T. (2016). Cilia have high cAMP levels that are inhibited by Sonic Hedgehog-regulated calcium dynamics. Proc. Natl. Acad. Sci. U. S. A. *113*, 13069–13074.

96. Chen, Q., Plasencia, M., Li, Z., Mukherjee, S., Patra, D., Chen, C.-L., Klose, T., Yao, X.-Q., Kossiakoff, A.A., Chang, L., et al. (2021). Structures of rhodopsin in complex with G-protein-coupled receptor kinase 1. Nature. 10.1038/s41586-021-03721-x.

97. Taylor, S.S., Herberg, F.W., Veglia, G., and Wu, J. (2023). Edmond Fischer's kinase legacy: History of the protein kinase inhibitor and protein kinase A. IUBMB Life. 10.1002/iub.2714.

98. Taylor, S.S., Zhang, P., Steichen, J.M., Keshwani, M.M., and Kornev, A.P. (2013). PKA: lessons learned after twenty years. Biochim. Biophys. Acta *1834*, 1271–1278.

99. Taylor, S.S., Ilouz, R., Zhang, P., and Kornev, A.P. (2012). Assembly of allosteric macromolecular switches: lessons from PKA. Nat. Rev. Mol. Cell Biol. *13*, 646–658.

100. Kliewer, A., Reinscheid, R.K., and Schulz, S. (2017). Emerging Paradigms of G Protein-Coupled Receptor Dephosphorylation. Trends Pharmacol. Sci. *38*, 621–636.

101. Zhao, L., Wang, L., Chi, C., Lan, W., and Su, Y. (2017). The emerging roles of phosphatases in Hedgehog pathway. Cell Commun. Signal. *15*, 35.

102. Scamfer, S.R., Lee, M.D., and Hilgendorf, K.I. (2022). Ciliary control of adipocyte progenitor cell fate regulates energy storage. Front. Cell Dev. Biol. *10*, 1083372.

103. Mahoney, J.P., Bruguera, E.S., Vasishtha, M., Killingsworth, L.B., Kyaw, S., and Weis, W.I. (2022). PI(4,5)P2-stimulated positive feedback drives the recruitment of Dishevelled to Frizzled in Wnt-β-catenin signaling. Sci. Signal. *15*, eabo2820.

104. Patil, D.N., Singh, S., Laboute, T., Strutzenberg, T.S., Qiu, X., Wu, D., Novick, S.J., Robinson, C.V., Griffin, P.R., Hunt, J.F., et al. (2022). Cryo-EM structure of human GPR158 receptor coupled to the RGS7-Gβ5 signaling complex. Science *375*, 86–91.

105. Orlandi, C., Xie, K., Masuho, I., Fajardo-Serrano, A., Lujan, R., and Martemyanov, K.A. (2015). Orphan Receptor GPR158 Is an Allosteric Modulator of RGS7 Catalytic Activity with an Essential Role in Dictating Its Expression and Localization in the Brain*♦. J. Biol. Chem. *290*, 13622–13639.

106. Cao, W., Luttrell, L.M., Medvedev, A.V., Pierce, K.L., Daniel, K.W., Dixon, T.M., Lefkowitz, R.J., and Collins, S. (2000). Direct binding of activated c-Src to the beta 3-adrenergic receptor is required for MAP kinase activation. J. Biol. Chem. *275*, 38131–38134.